THE JOURNAL OF PHYSICAL CHEMISTRY Letters

Letter

pubs.acs.org/JPCL

Effects of Solute–Solvent Hydrogen Bonding on Nonaqueous Electrolyte Structure

Kjell W. Schroder,[†,‡] Anthony G. Dylla,[‡] Logan D. C. Bishop,[‡] Elizabeth R. Kamilar,[‡] Jennette Saunders,[‡] Lauren J. Webb,*[,†,‡] and Keith J. Stevenson*[,†,‡]

[†]Materials Science and Engineering Program, Texas Materials Institute, University of Texas at Austin, 204 East Dean Keeton Street, Stop C2201, Austin, Texas 78712, United States

[‡]Department of Chemistry and Center for Nano- and Molecular Science, University of Texas at Austin, 1 University Station/MC A5300, Austin, Texas 78712, United States

Supporting Information

ABSTRACT: We investigate the source of Raman background signal commonly misidentified as fluorescence in nonaqueous electrolytes via a variety of spectroscopies (Raman, fluorescence, NMR) and find evidence of hydrogen-bonding interactions. This hydrogen bonding gives rise to broadband anharmonic vibrational modes and suggests that anions play an important and underappreciated role in the structure of nonaqueous electrolytes. Controlling electrolyte structure has important applications in advancing in operando spectroscopy measurements as well as understanding the stability of high concentration electrolytes for next-generation electrochemical energy storage devices.

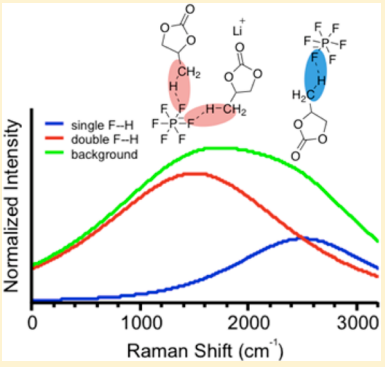

Downloaded by UNIV OF TEXAS AT AUSTIN on August 27, 2015 | http://pubs.acs.org
Publication Date (Web): July 10, 2015 | doi: 10.1021/acs.jpclett.5b01216

Nonaqueous electrolytes are essential to many next-generation electrochemical energy storage technologies, including supercapacitors, lithium-ion batteries (LIBs), sodium-ion batteries, lithium–air batteries, lithium–sulfur batteries, and redox flow batteries. Their importance comes from their solvents' wide electrochemical window of stability, enabling the use of redox couples with potentials not accessible or stable in aqueous media.[1−3]

Raman spectroscopy has become a ubiquitous tool to study the structure of electrode materials and solution species (e.g., redox shuttles in flow batteries or additives in LIBs) in these electrolytes.[4] Raman reports on bulk solid and liquid materials properties (e.g., bonding, ion solvation) and surface properties via vibrational modes. Most reports of electrochemical materials focus on post hoc, ex situ characterization of single device components (electrode or electrolyte), but these results are difficult to interpret because this approach may leave artifacts and miss important whole-system level interactions. Raman spectra taken during operation of a device (in operando) or immediately after without cell/device deconstruction (in situ) are promising methods to investigate surface and bulk materials properties, in addition to being nondestructive and inexpensive.[4,5]

Raman is often limited in nonaqueous systems by the presence of large background signals. This background is commonly associated with (1) high ion concentration electrolytes or (2) high polarization potentials at an electrode's surface during in operando measurements. Consequently, peaks of interest (i.e., vibrational modes of electrode materials or electrolytes) have low signal-to-noise even after background removal, inhibiting the observation of particular vibrational modes during electrochemical reactions (e.g., lithiation of a material or formation of an SEI species).

This background is commonly misattributed to fluorescence. Reports rarely identify explicit fluorophores or conclusively characterize the electrochemical system of interest to determine the source of the background. In one recent exception, Norberg, Kosetcki, and coworkers[6] have shown that disproportioned and solubilized manganese (e.g., from a LIB cathode material) can coordinate with solvent molecules and degrade solvent products to form fluorescent complexes; however, barring this study, persistent errors have been propagated in the literature regarding the origin of this background, which we explore in detail.

Figure 1 shows examples of Raman spectra of neat solutions, which have never been in contact with an electrode, let alone undergone electrochemistry. Figure 1a comprises spectra of both lithium and sodium ion salts in propylene carbonate (PC) at 1 M concentration. In all of these cases, the background shows a Voigt (Gaussian–Lorentzian) character, and treating the backgrounds as broad peaks, (normalized relative to the most intense C–H stretching mode at ∼2900 cm^{-1}), their

Received: June 8, 2015
Accepted: July 8, 2015
Published: July 8, 2015

 © 2015 American Chemical Society

DOI: 10.1021/acs.jpclett.5b01216
J. Phys. Chem. Lett. 2015, 6, 2888−2891

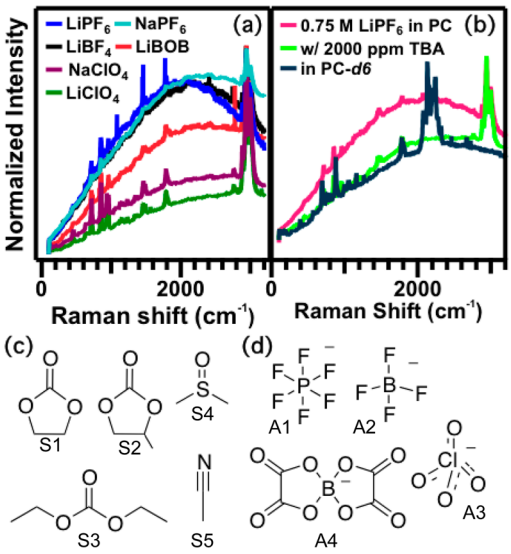

Figure 1. Raman spectra of 1 M PC-based electrolytes with sodium and lithium salts (a) and Raman spectra of 0.75 M $LiPF_6$ in PC (pink), 0.75 M $LiPF_6$ in PC with 2000 ppm TBA (neon green), and 0.75 M $LiPF_6$ in PC-d_6 (slate) (b). All spectra normalized to C−H stretching at ∼2900 cm^{-1}. Structural drawings of solvents (c) PC (S1), EC (S2), DEC (S3), DMSO (S4), and acetonitrile (S5) as well as anions (d) PF_6^- (A1), BF_4^- (A2), ClO_4^- (A3), and bis(oxalato)borate (BOB^-) (A4) are shown for reference.

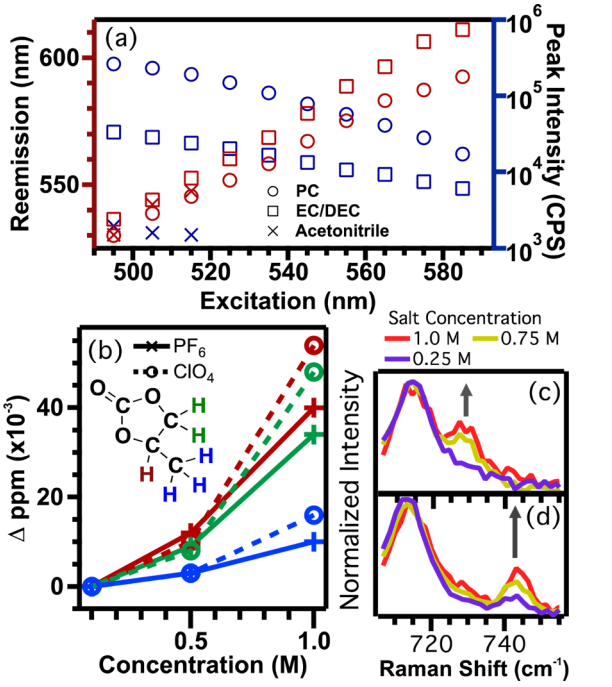

Figure 2. Fits of emission spectra peaks (a) of 1 M $LiPF_6$ in PC, 1:1 EC/DEC (by wt %) and acetonitrile as a function of excitation energy. The excitation energy is plotted versus the reemission peak energy (left axis, red) and peak intensity (right axis, blue). ^1H NMR (b) of solvent hydrogen atoms (red, green, blue) in solutions of $LiPF_6$ (solid, pluses) and $LiClO_4$ (dashed, circles) in 20:1 PC:PC-d_6. Raman spectra of PC solutions of LiBOB (c) and $LiPF_6$ (d) at different concentrations (purple, gold, red); spectra were normalized to the peak at ∼715 cm^{-1} and background-subtracted.

intensity and center are dependent on the anion and cation in solution.

Changing the properties of the hydrogen on the solvent molecule also affects this broad Raman peak. In Figure 1b, 0.75 M $LiPF_6$ in PC is compared with the same solution with the addition of a nucleophile (tributylamine, TBA) and 0.75 M $LiPF_6$ in deuterium-labeled PC (PC-d_6). The background intensity of the PC-d_6 solution decreased and blue-shifted relative to the control measurement and the C−D stretching modes are red-shifted to ∼2100 cm^{-1}, as expected (compared with ∼3000 cm^{-1} for C−H stretching). A change in the isotopic makeup of the solvent does not affect the electronic states of the molecule; however, it does affect the vibrational states. Therefore, the background is not likely due to an electronic transition (fluorescence). Figure 1b also includes a Raman spectrum of 2000 ppm TBA in 0.75 M $LiPF_6$. TBA is known to quench fluorescence;[7] instead, we observed a blue shift in the background and a decrease in intensity relative to the control, similar to the PD-d_6. Both of these results suggest that hydrogen is involved in the background phenomena and that it is not due to fluorescence.

To further investigate the mechanism that leads to this behavior, we performed a series of complementary spectroscopic experiments. Figure 2a shows emission peak wavelength as a function of excitation wavelength for 1 M $LiPF_6$ solutions in PC, 1:1 EC/DEC (by wt %) and acetonitrile. (For reasons having to do with the fitting discussed in the Supporting Information (SI), 10 excitations were studied for the carbonates and 3 for acetonitrile.) These spectra (e.g., Figure S5 in the SI) showed similar Voigt character to the background in the Raman spectra of Figure 1a,b. A fluorescence process would imply the observed reemission peak would be at the same energy, regardless of the excitation wavelength used to probe the sample. Instead, the reemission peaks follow a monotonic increase with excitation energy, implying the peak results from Raman scattering, not fluorescence. While a more detailed exploration of the Raman excitation wavelength dependence is outside the scope of this work, it should be noted that lower energy excitation would likely not provide a clearer picture of the mechanism at play. Figure S5 in the SI shows that the emission peak intensity rapidly diminishes at wavelengths longer than 600 nm. On the basis of this result, we would expect a diminished background character to spectra collected with a lower energy excitation source such as 1064 nm, but this would not indicate that we moved outside of the range of fluorescence, only that we moved outside of the range of the broad Raman scattering peak.

To investigate how anion concentration and anion identity affects the hydrogen in PC, ^1H NMR spectra of $LiPF_6$ and $LiClO_4$ were taken at three different concentrations in 20:1, PC:PC-d_6. Multiplets were assigned to particular hydrogen atoms, and their peak shifts, relative to their positions at 0.1 M, are plotted in Figure 2b. In general ^1H peaks shifted downfield (to higher frequency) with increasing concentration of salt; we attribute this to the higher solution conductivity (lessening of signal attenuation). Proton shifts from PF_6^- were equal to or greater than shifts from ClO_4^- at 0.5 M, but at higher concentrations, shifts from PF_6^- were all less than those from ClO_4^-. Only three interactions could have caused this behavior: ion−ion, solvent−solvent, and solvent−ion. In PC, lithium is coordinated by the carbonyl;[2,8] therefore, ion−ion interactions (ion pairing) should have no effect on the local shielding of solvent protons, which are far from the carbonyl. If a decreasing fraction of solvent molecules participated in solvent−solvent hydrogen bonds with increasing salt concentration, this might

Downloaded by UNIV OF TEXAS AT AUSTIN on August 27, 2015 | http://pubs.acs.org
Publication Date (Web): July 10, 2015 | doi: 10.1021/acs.jpclett.5b01216

DOI: 10.1021/acs.jpclett.5b01216
J. Phys. Chem. Lett. 2015, 6, 2888−2891

Downloaded by UNIV OF TEXAS AT AUSTIN on August 27, 2015 | http://pubs.acs.org
Publication Date (Web): July 10, 2015 | doi: 10.1021/acs.jpclett.5b01216

explain the NMR results; however, this is inconsistent with the observations that hydrogen is involved in the vibrational mode detected by Raman scattering (Figure 1b) and the fact that this interaction is stronger with PF_6^- than ClO_4^- (Figure 1a). Solvent−anion hydrogen bonding explains the increased shielding (Figure 2b) because C−H−F hydrogen bonds are known to involve C−H bond contraction,[9,10] and thus result in increased proton shielding (less downfield shift relative to ClO_4^-).

Secondary effects of the anion-solvent hydrogen bonding are also observable in the skeletal deformation mode of PC (observed unperturbed at ∼715 cm^{-1}). Figure 2c,d shows Raman spectra of three neat solutions of LiBOB in PC and $LiPF_6$ in PC, respectively. The perturbed solvent peak grows with concentration of LiBOB at ∼730 cm^{-1} (Figure 2c) compared with ∼740 cm^{-1} for $LiPF_6$ in PC (Figure 2d). The perturbation of this skeletal deformation mode of PC is most often attributed to the carbonyl interaction with Li^+ upon solvation. Because both salts include Li^+ at the same concentrations, the increased blue shift in the $LiPF_6$ spectra (relative to the LiBOB) is due to stronger anion−solvent inactions. Returning to Figure 1a, LiBOB showed blue-shifted and decreased background intensity, compared with $LiPF_6$.

We are left concluding that anions, particularly fluorinated ions or species with at least one lone pair (TBA, BOB^-), have a strong interaction with solvent hydrogen atoms (e.g., the hydrogen atoms of the propylene group in PC). This is apparent in the Raman background, NMR, and the emission spectra as well as indirectly via the Stark effect observations (perturbed-solvent deformation mode) shown in Figure 2c,d. In Figure 3, we further quantify this hydrogen-bond interaction. Figure 3a shows spectra of solutions of $LiPF_6$ in PC. Fitting the data with pseudo-Voigt functions shows trends in both the peak center red shifting and growing intensity with concentration (Figure 3b).

The anharmonic vibrational mode that results from the hydrogen bonding is caused either through coupling of existing solvent and ion modes[11] or through the strongly anharmonic potential of the hydrogen bond itself.[10,12] Figure 3c comprises an illustration of these hydrogen-bonding interactions, consistent with our observations. As anion concentration increases, there is a greater population of hydrogen bonds, leading to the increase in background intensity. A greater population of anions participating in more than one hydrogen bond interaction explains the red shift; resulting delocalized electron density on the anion causes bond lengthening and red shifting of the background. In this way, the anion acts to structure the electrolyte.

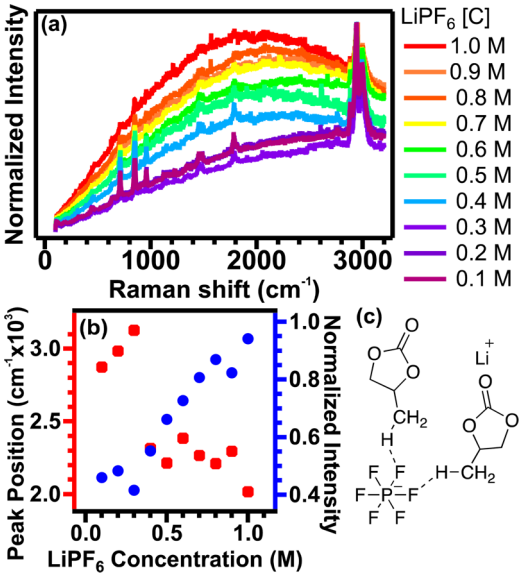

Figure 3. Raman spectra of solutions of $LiPF_6$ in PC (a) and a summary of the intensities and peak positions of the backgrounds of these spectra from Voigt fitting (b). An illustration of the PF_6^--PC hydrogen bonding interactions (c).

The results clearly show that fluorescence is not the cause of low signal-to-noise Raman data taken during in operando and in situ experiments. If it were, a laser with lower energy wavelength would eliminate the background, but these results imply that while lower excitation energies minimize the background intensity they do not eliminate the effect. Additionally, adding quenchers (such as TBA) suppress the background, but they also disrupt the structure of the electrolyte, as seen by the effect of the TBA inhibiting PF_6^-−PC interactions (Figure 2b).

These results also have implications on the mechanisms involved in stabilizing electrolytes. Recently Yamada et al. have demonstrated that high concentration electrolytes have reduced decomposition on graphite with cycling, even when used in conjunction with typically unstable or cointercalating electrolytes (i.e., PC, acetonitrile, DMSO).[13,14] The results we have shown here suggest that the stability can come from the anion interactions with the solvent. In this case, absolute concentration is not as important as the degree of interaction between anion and solvent (for an electrolyte with a given working cation). This sheds light on why the $TFSI^-$ anion (which has many possible hydrogen bond acceptors) was shown to be so stable at high concentrations by Yamada et al. in nontraditional battery electrolytes. Additionally, electrolyte additives like LiBOB and fluoroethylene carbonate (FEC) have been shown to affect solid electrolyte interface formation in LIBs and sodium ion batteries.[1−3] The effectiveness of these species as additives is usually given in terms of their stable, insoluble decomposition products that coat an electrode's surface; however, our results suggest that their effect on the electrolyte structure is also of critical importance.

EXPERIMENTAL METHODS

Solution Preparation. All solutions were prepared inside a glovebox (Innovative Technologies) with <8 ppm of O_2 and 1 ppm of H_2O. Propylene carbonate (Arcos), six-deuterium propylene carbonate (PC-d_6, CDN isotopes), ethylene carbonate and diethyl carbonate blend (1:1 by wt %, BASF), acetonitrile (Sigma-Aldrich), dimethyl sulfoxide (Arcos), LiBOB (Rockwood Lithium), and $LiPF_6$ (BASF) were used as received (under argon). $LiClO_4$ and $LiBF_4$ (Sigma-Aldrich) were transferred into the glovebox after heating in a vacuum oven at 100 °C for 90 min to remove any excess water.

Prior to mixing solutions, the glovebox was purged with high-purity argon gas (99.999999% pure, Praxair) for 1 min to remove possible gaseous contaminants. All solutions were prepared by creating a high molarity (typically 1.0 M) solution and stirring until the salt was fully dissolved. From this parent solution, a series of dilutions were made. All solutions were stored in plastic containers in the glovebox. Solution samples reserved for spectroscopy were sealed in either 1 mL cylindrical glass vials (Fisher Scientific) or 5 mm glass NMR tubes

DOI: 10.1021/acs.jpclett.5b01216
J. Phys. Chem. Lett. 2015, 6, 2888−2891

(Wilmad Glasslab) with their caps wrapped with parafilm. As a control, a piece of sodium was sealed in a similar fashion and remained visibly metallic for 4 days; however, PF_6^- and BF_4^- solutions stored in glass expressed color change from clear to reddish-brown over 24−36 h; samples were discarded after 12 h stored in glass.

Raman Spectroscopy. Analysis of the solutions was performed using a long-range 50× objective on a confocal Raman microscope spectrophotometer (Renishaw, InVia, controlled by WiRE v. 4.x software). Typical laser powers reached 15 mW at full intensity; measurements were taken at 5% power using a 514.5 nm Ar^+ excitation source through restricting both the laser tube power and neutral density filters within the instrument. All solutions were scanned for 5 min accumulations from 0 to 3300 cm^{-1}, and all scans took place within 6 h of mixing the solution.

Data analysis was performed using Igor Pro (v.6.36 WaveMetrics). Gaussian fits were made using the TN020 procedure file from Igor Pro. When the data were baseline-corrected (e.g., Figure 2c,d), the parametrized Gaussian fit functions were subtracted from the raw spectra. All spectra were normalized against the highest peak (C−H stretching mode at ∼2900 cm^{-1}).

Spectra taken at known concentrations of $LiPF_6$ in PC (data of Figure 3a, reprinted in Figure S1a in the SI) may be compared with the Gaussian fits of the background of the same data (Figure S1b in the SI). The analysis of these fits−the position of their maximums and the normalized intensity of their maximums−was the information used to construct Figure 3b. As noted in the manuscript, the background shows a clear red shift and growing intensity with increasing concentration of salt.

■ ASSOCIATED CONTENT

Supporting Information

Raman spectra fits, ^{13}C, ^{18}F, ^{31}P NMR spectra, and emission spectra of electrolytes. The Supporting Information is available free of charge on the ACS Publications website at DOI: 10.1021/acs.jpclett.5b01216.

■ AUTHOR INFORMATION

Corresponding Authors

*E-mail: stevenson@cm.utexas.edu (K.J.S.).
*E-mail: lwebb@cm.utexas.edu (L.J.W.).

Notes

The authors declare no competing financial interest.

■ ACKNOWLEDGMENTS

This material is based on work supported as part of the program "Understanding Charge Separation and Transfer at Interfaces in Energy Materials (EFRC:CST)," an Energy Frontier Research Center funded by the U.S. Department of Energy, Office of Science, Office of Basic Energy Sciences under Award Number DE-SC0001091. L.D.C.B. acknowledges the generous support of the Beckman Foundation.

■ REFERENCES

(1) Xu, K. Electrolytes and Interphasial Chemistry in Li Ion Devices. *Energies* **2010**, *3*, 135−154.
(2) Xu, K. Nonaqueous Liquid Electrolytes for Lithium-Based Rechargeable Batteries. *Chem. Rev.* **2004**, *104*, 4303−4417.
(3) Xu, K. Electrolytes and Interphases in Li-Ion Batteries and Beyond. *Chem. Rev.* **2014**, *114*, 11503−11618.
(4) Baddour-Hadjean, R.; Pereira-Ramos, J.-P. Raman Microspectrometry Applied to the Study of Electrode Materials for Lithium Batteries. *Chem. Rev.* **2010**, *110*, 1278−1319.
(5) Stancovski, V.; Badilescu, S. In Situ Raman Spectroscopic−Electrochemical Studies of Lithium-Ion Battery Materials: A Historical Overview. *J. Appl. Electrochem.* **2014**, *44*, 23−43.
(6) Norberg, N. S.; Lux, S. F.; Kostecki, R. Interfacial Side-Reactions at a LiNi0.5Mn1.5O 4 Electrode in Organic Carbonate-Based Electrolytes. *Electrochem. Commun.* **2013**, *34*, 29−32.
(7) Wang, Y. Quenching of Singlet and Triplet States of p-N,N-Dimethylaminobenzonitrile by Tertiary Amines. Intramolecular Charge-Transfer State and Excited-State Three-Electron Bond. *J. Chem. Soc., Faraday Trans. 2* **1988**, *84*, 1809−1823.
(8) Bogle, X.; Vazquez, R.; Greenbaum, S.; Cresce, A. V. W.; Xu, K. Understanding Li^+−Solvent Interaction in Nonaqueous Carbonate Electrolytes with ^{17}O NMR. *J. Phys. Chem. Lett.* **2013**, *4*, 1664−1668.
(9) Karpfen, A.; Kryachko, E. S. Blue-Shifted Hydrogen-Bonded Complexes. II. $CH_3F\cdots(HF)_{1\leqslant n\leqslant 3}$ and $CH_2F_2\cdots(HF)_{1\leqslant n\leqslant 3}$. *Chem. Phys.* **2005**, *310*, 77−84.
(10) Hobza, P.; Havlas, Z. Blue-Shifting Hydrogen Bonds. *Chem. Rev.* **2000**, *100*, 4253−4264.
(11) Ostrovskii, D.; Yaremko, A.; Vorona, I. Nature of Background Scattering in Raman Spectra of Materials Containing High-Wavenumber Vibrations. *J. Raman Spectrosc.* **1997**, *28*, 771−778.
(12) Fontaine-Vive, F.; Johnson, M. R.; Kearley, G. J.; Howard, J. a K.; Parker, S. F. How Phonons Govern the Behavior of Short, Strong Hydrogen Bonds in Urea-Phosphoric Acid. *J. Am. Chem. Soc.* **2006**, *128*, 2963−2969.
(13) Yamada, Y.; Furukawa, K.; Sodeyama, K.; Kikuchi, K.; Yaegashi, M.; Tateyama, Y.; Yamada, A. Unusual Stability of Acetonitrile-Based Superconcentrated Electrolytes for Fast-Charging Lithium-Ion Batteries. *J. Am. Chem. Soc.* **2014**, *136*, 5039−5046.
(14) Yamada, Y.; Usui, K.; Chiang, C. H.; Kikuchi, K.; Furukawa, K.; Yamada, A. General Observation of Lithium Intercalation into Graphite in Ethylene-Carbonate-Free Superconcentrated Electrolytes. *ACS Appl. Mater. Interfaces* **2014**, *6*, 10892−10899.

Downloaded by UNIV OF TEXAS AT AUSTIN on August 27, 2015 | http://pubs.acs.org
Publication Date (Web): July 10, 2015 | doi: 10.1021/acs.jpclett.5b01216

DOI: 10.1021/acs.jpclett.5b01216
J. Phys. Chem. Lett. 2015, 6, 2888−2891